Depositional environments of the Yeso Formation (Lower Permian), southern Caballo Mountains, New Mexico

Greg H. Mack and Suguio Kenitiro

New Mexico Geology, v. 13, n. 3 pp. 45-49, 59, Print ISSN: 0196-948X, Online ISSN: 2837-6420.
https://doi.org/10.58799/NMG-v13n3.45

New Mexico Bureau of Geology & Mineral Resources
New Mexico Institute of Mining & Technology
801 Leroy Place
Socorro, NM 87801-4796

https://geoinfo.nmt.edu

This page is intentionally left blank to maintain order of facing pages.

New Mexico GEOLOGY
• Science and Service
ISSN 0196-948X
Volume 13, No. 3, August 1991

Depositional environments of the Yeso Formation (Lower Permian), southern Caballo Mountains, New Mexico

by *Greg H. Mack*, New Mexico State University, Las Cruces, NM 88003
and *Kenitiro Suguio*, Univ. de Sao Paulo, C.P. 20.899, Sao Paulo, Brazil

Introduction

The Yeso Formation in south-central New Mexico occupies a stratigraphic position above nonmarine redbeds of the Abo Formation and below shallow-marine limestones of the San Andres Formation (Kottlowski et al., 1956; Kottlowski, 1963, 1965; Nelson, 1986). Despite a general consensus that the Yeso represents a transitional period of shallow-marine and shoreline sedimentation, there have been few detailed sedimentological studies. We present here an interpretation of Yeso depositional environments based on outcrops in the southern Caballo Mountains (Fig. 1). Although small in area, the southern Caballo Mountains provide excellent exposures of the Yeso Formation, particularly of the basal Meseta Blanca Member. The model presented here hopefully can be used as a standard of comparison for other Yeso outcrops in southern New Mexico.

Stratigraphy

The Yeso Formation in the southern Caballo Mountains has been divided by Seager and Mack (in press) into four members, which in ascending order are the Meseta Blanca, red siltstone–dolomite, limestone, and sandstone–limestone (Fig. 2). The Meseta Blanca Member in the southern Caballo Mountains is similar in appearance to the one at the type section in the Oscura Mountains (Wilpolt and Wanek, 1951). The other three members are sufficiently different from those of the type section to warrant a new stratigraphic terminology.

The Meseta Blanca Member in the southern Caballo Mountains is approximately 75 m thick and has conformable upper and lower contacts. The lower contact is marked by a change over a meter or less from interbedded red mudstone and ledge-forming siltstone of the Abo Formation to orangish-red, friable sandstones. The Meseta Blanca Member consists primarily of medium- and thin-bedded, very fine sandstone, although a few thin (≤4 m) beds of gray shale and tan dolomite may be present in the upper 15 m.

In the western part of the study area, the red siltstone–dolomite member is 72 m thick and is composed of interbedded tan dolomite, gray limestone, red siltstone to fine sandstone, and white fine-grained sandstone. The member increases significantly in thickness toward the eastern part of the study area where it attains a maximum thickness of 196 m (Fig. 2). The increase in thickness is due almost entirely to the presence of gypsum.

The limestone member conformably overlies the red siltstone–dolomite member and forms a prominent ridge wherever exposed throughout the southern Caballo Mountains. Approximately 25 m thick, the limestone member consists of thin-bedded, dark-gray, fossiliferous limestone. Dark chert nodules are present and some of the fossils are silicified. Kelley and Silver (1952) mapped

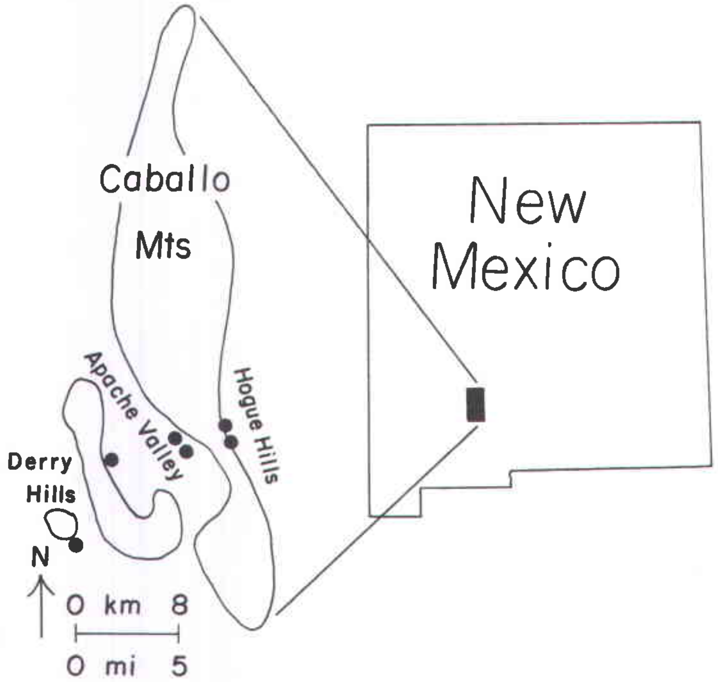

FIGURE 1—Location of Caballo Mountains in south-central New Mexico. Closed circles represent location of measured sections.

Also in this issue

Coming soon

1990 discovery wells
Coal-bed methane in New Mexico
Earth fissures of the Mimbres Basin

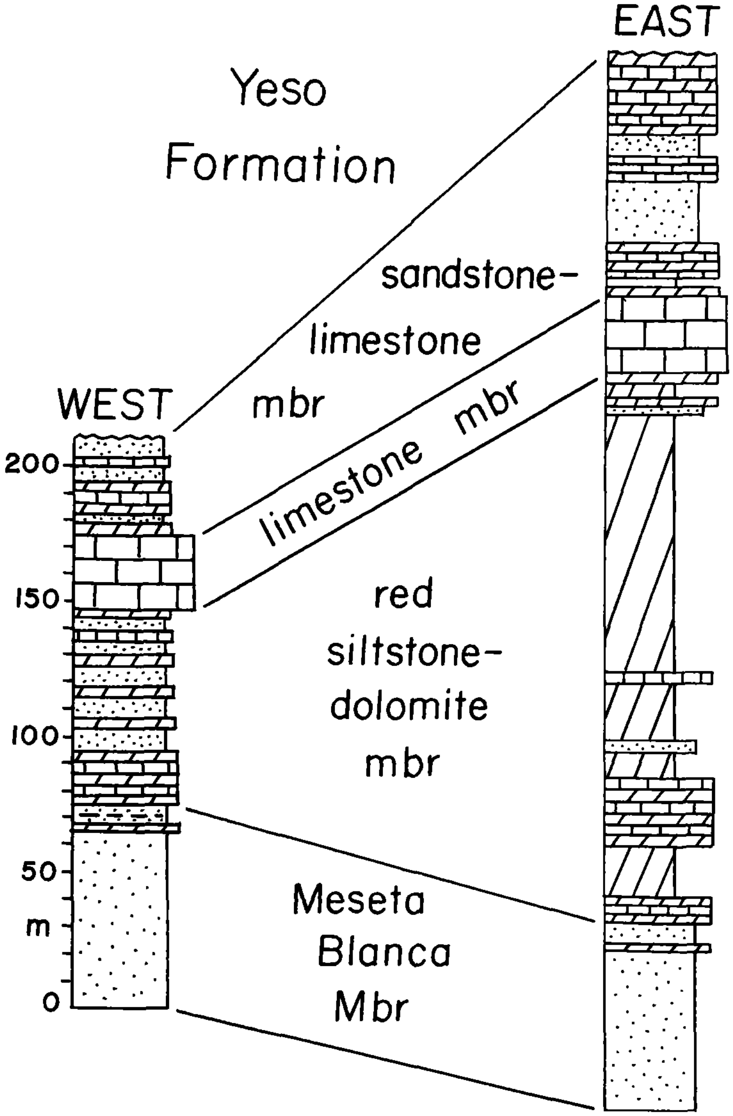

FIGURE 2—Simplified stratigraphic columns of the Yeso Formation in the southern Caballo Mountains. "East" refers to the Hogue Hills and "West" refers to Apache Valley. Only part of the Meseta Blanca Member is exposed near the Derry Hills.

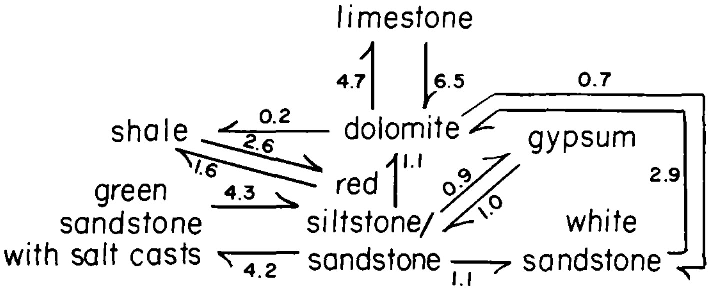

FIGURE 3—Lithofacies relationship diagram based on a Markov analysis described by Harms et al. (1975). Arrows show probable vertical lithofacies transitions. The higher the number associated with an arrow, the greater the probability that the vertical transition is not random. Total number of observed vertical transitions is 127.

this member and the overlying member as the San Andres Formation, a convention that is not considered accurate by Seager and Mack (in press).

Conformably overlying the limestone member is the sandstone–limestone member, which ranges from 43 m thick in the western part of the study area to 100 m thick in the eastern part. The variation in thickness is largely due to relief on the unconformity that separates the Yeso and Cretaceous Dakota Formations (Seager and Mack, in press). The sandstone–limestone member has the same suite of rock types as the red siltstone–dolomite member, but contains fewer beds of red siltstone and sandstone and more beds of fossiliferous limestone.

Description of lithofacies

The Yeso Formation in the southern Caballo Mountains is composed of seven lithofacies that are interbedded on a scale of less than one meter to tens of meters. In order to more accurately define vertical lithofacies relationships, a Markov statistical analysis was performed with data from two measured sections (Fig. 3).

New Mexico GEOLOGY
• Science and Service
ISSN 0196-948X
Volume 13, No. 3, August 1991
Editor: Carol A. Hjellming
Drafting Assistance: Kathryn Campbell
Published quarterly by
New Mexico Bureau of Mines and
Mineral Resources
a division of New Mexico Institute of
Mining & Technology

Subscriptions: Issued quarterly, February, May, August, November; subscription price $6.00/calendar year.
Editorial matter: Articles submitted for publication should be in the editor's hands a minimum of five (5) months before date of publication (February, May, August, or November) and should be no longer than 20 typewritten, double-spaced pages. All scientific papers will be reviewed by at least two people in the appropriate field of study. Address inquiries to Carol A. Hjellming, Editor of *New Mexico Geology*, New Mexico Bureau of Mines & Mineral Resources, Socorro, NM 87801-4796.
Published as public domain, therefore reproducible without permission. Source credit requested.
Circulation: 1,600
Printer: University of New Mexico Printing Services

Red siltstone–sandstone lithofacies

Medium to thin beds of red, very well sorted siltstone or very fine to fine-grained sandstone constitute the majority of the Meseta Blanca Member (90%) and lesser amounts of the red siltstone–dolomite (9%) and sandstone–limestone (6%) members. The dominant sedimentary structures are horizontal and low-angle laminae, which are composed of small-scale climbing ripples (Fig. 4a, b). The ripples are asymmetrical and are characterized by low amplitude (≤5 mm) and high ripple index (~100). Foreset laminae are rare, but generally a few are visible within the length of the ripple (Fig. 4b). In some cases the ripple laminae exhibit inverse grading (Fig. 4c). In plan view, the ripples are straight to sinuous and commonly bifurcate. Bioturbation is also common and consists of small (≤0.5 mm diameter, ≤5 cm length), straight to sinuous forms. The degree of bioturbation varies from bed to bed and is least well developed in the Meseta Blanca Member. Desiccation cracks, small-scale (≤20 cm) crossbeds, salt casts, and soft sediment folds and faults are much less common in this lithofacies.

Fine grain size, excellent sorting, and abundance of low-amplitude climbing ripples suggest an eolian origin for the red siltstone–sandstone lithofacies. Climbing ripples in the Yeso are similar to subcritically climbing wind ripples described in modern eolian deposits (Hunter, 1977; Fryberger et al., 1979) and those produced in wind tunnel experiments (Fryberger and Schenk, 1981). Particularly diagnostic are subcritical angle of climb (≤10°), low amplitude, high ripple index, inverse grading, and the paucity of foresets. Bioturbation is also common in modern eolian deposits dominated by climbing wind ripples (Ahlbrandt et al., 1978; Fryberger et al., 1979).

White sandstone lithofacies

Thin- to medium-bedded white sandstone makes up two percent of the red siltstone–dolomite member and six percent of the sandstone–limestone member. The white sandstone lithofacies is distinguished from the red siltstone–sandstone lithofacies by color and by a slightly coarser grain size, although the two lithofacies contain some of the same sedimentary structures, including low-amplitude climbing ripples and bioturbation. The white sandstone lithofacies also contains straight to sinuous, relatively large amplitude (≥1 cm), symmetrical ripples and larger scale (1 cm diameter, 1 cm length) sinuous to bifurcating horizontal burrows.

The presence of climbing wind ripples indicates that at least some beds of white sandstone are eolian in origin. However, symmetrical oscillation ripples and intercalation with beds that are interpreted as lagoonal gypsum suggest a shallow-marine or shoreline origin (Fig. 3).

Green sandstone lithofacies

Green sandstone constitutes only a small percentage of the Meseta Blanca Member (3%) and is exclusively interbedded with the red siltstone/sandstone lithofacies. Each bed is relatively thin (≤0.5 m) and consists of flaggy, very fine to fine-grained quartz sandstone. Particularly common are salt casts, desiccation cracks, and straight to sinuous, large-amplitude (0.5 to 1 cm), symmetrical ripple marks. The suite of sedimentary structures and association with the red siltstone–sandstone lithofacies suggest that green sandstone was deposited in small playa lakes dispersed across the eolian field.

Dolomite lithofacies

Thin to medium beds of tan dolomite from 0.5 to 4.0 m thick are a common component of the red siltstone–dolomite member (17%) and the sandstone–limestone member (16%). A few beds of dolomite are also present near the top of the Meseta Blanca Member. The dolomites are very fine grained and commonly display thin horizontal laminae that resemble cryptalgal laminae. LLH stromatolites and fenestral fabric also are common, as are small-scale brecciation and bioturbation. Less common are larger scale breccias, referred to as monogenic breccias by Bosellini and Hardie (1973), that consist of angular blocks up to one meter in diameter in a matrix of red siltstone or sparry calcite. The large-scale breccias probably resulted from dissolution of underlying evaporites. Also present in the dolomites are ripple cross-laminae and desiccation cracks (Fig. 4d). The suite of sedimentary structures present in the dolomite lithofacies is diagnostic of modern carbonate tidal flats (e.g. Shinn, 1983; James, 1984).

Limestone lithofacies

Thin- to medium-bedded, gray limestone makes up five percent of the red siltstone–dolomite member, 24 percent of the sandstone–limestone member, and all of the limestone member. The most common variety consists of fossiliferous packstone and wackestone containing brachiopods, corals, pelecypods, echinoderm columnals, bryozoa, gastropods, foraminifera, and phylloid algae (Fig. 4e). Bioturbation is common in this variety and some burrows are dolomitized. Abundant micrite matrix and highly diverse fauna, including many filter feeders, suggest a low-energy, normal-marine depositional environment.

Less common are wackestones composed of peloids and a low-diversity fauna of foraminifera, ostracods, and gastropods (Fig. 4f). This variety of limestone was probably deposited in a nearshore lagoon characterized by abnormal salinity and/or poor circulation.

Also included in the limestone lithofacies are several beds of ripple cross-laminated and crossbedded oolite grainstone. The absence of channels and subaerial exposure features suggests that oolite grainstone was deposited as subtidal shoals (e.g. Ball, 1967). In a few beds of limestone, recrystallization has destroyed all of the original textures, inhibiting interpretation of depositional environment.

Gypsum lithofacies

Gypsum composes approximately 70 percent of the red siltstone–dolomite member in the eastern part of the study area (Fig. 2). Gypsum is also present locally near the top of the Meseta Blanca Member and near the base of the sandstone–limestone member. Gypsum is white to light gray and is either massive or displays two different types of laminae. One type consists of thin (0.5 cm), discontinuous bands of vertically oriented coarse-grained gypsum crystals alternating with massive, fine-grained gypsum. The other type exhibits alternating thick (1 to 2 cm) light and thin (0.5 cm) dark laminae of fine-grained gypsum.

Gypsum exposed along the eastern flank of the southern Caballo Mountains marks the southwestern edge of a region of gypsum-rich strata that has a maximum thickness in excess of 600 m (Kottlowski, 1965). The combination of thick intervals of gypsum, which in the southern Caballo Mountains are up to 90 m, small-scale laminae, and the absence of nodular textures supports a lagoonal, rather than supratidal, origin for the gypsum (Kendall, 1984). However, this evidence is not conclusive, and geochemical data, particularly sulfur isotopes, would more accurately define the depositional environment (e.g. Thode et al., 1961; Sarg, 1981).

Shale lithofacies

Gray shale is the least common lithofacies in the Yeso Formation and is restricted to a few thin (0.5 to 4 m) beds near the top of the Meseta Blanca Member. Although too poorly exposed to confidentally interpret the depositional environment, the fact that the shale is interbedded with red siltstone–sandstone and dolomite lithofacies suggests a nearshore environment (Fig. 3).

☞

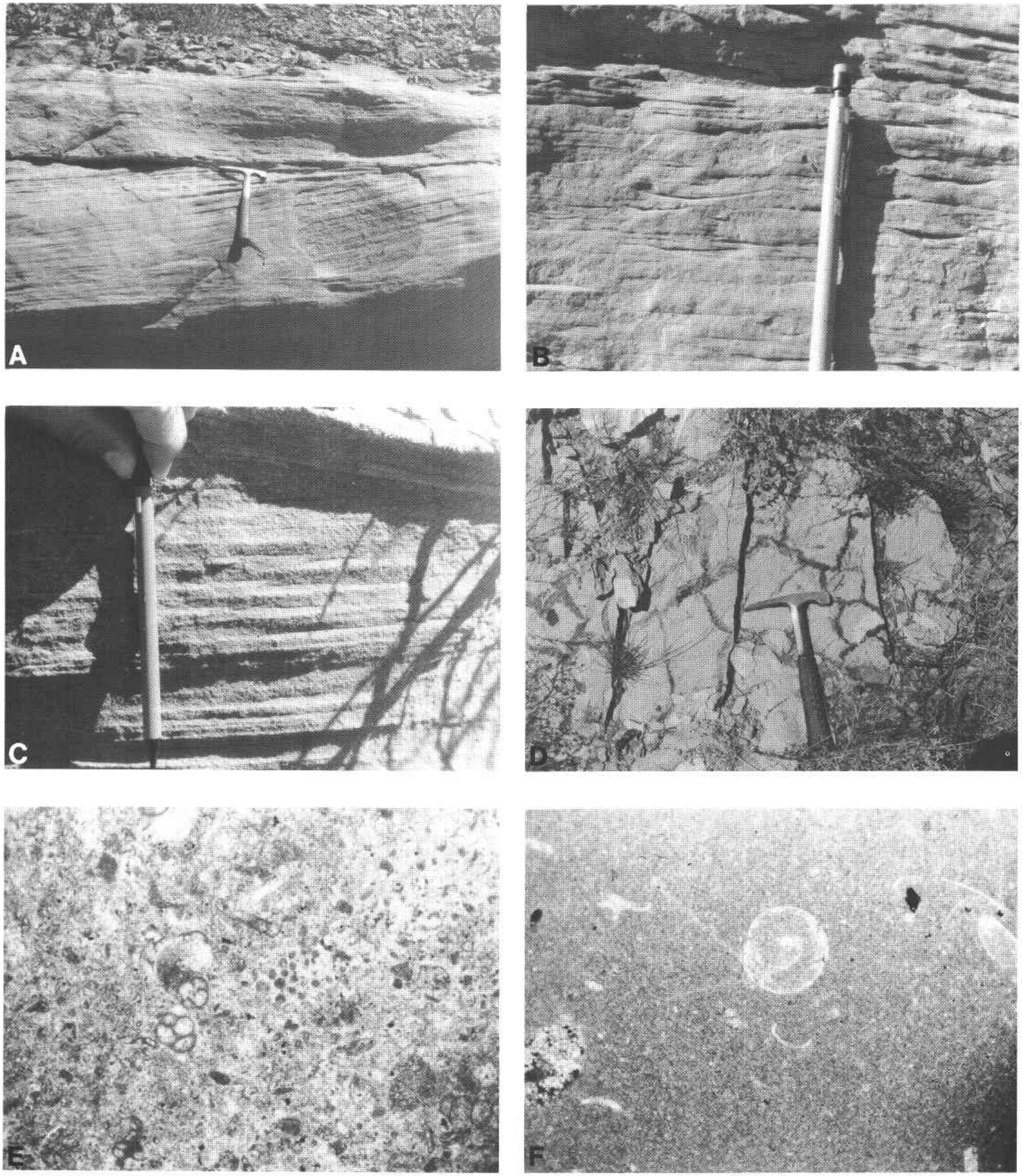

FIGURE 4—Lithofacies of the Yeso Formation in the southern Caballo Mountains. **A,** very fine to fine-grained sandstone of the Meseta Blanca Member displaying horizontal and low-angle laminae, which represent subcritically climbing wind ripples. Hammer is 25 cm long. **B,** climbing wind ripples in very fine sandstone of the Meseta Blanca Member. Pen is 15 cm long. **C,** climbing wind-ripple laminae exhibiting inverse grading. Recessed areas are finer grained than the microledges; Meseta Blanca Member. Pen is 15 cm long. **D,** bedding plane of dolomite showing desiccation cracks filled with gypsum; sandstone–limestone member. Hammer is 25 cm long. **E,** photomicrograph of packstone with highly diverse fauna, limestone member. Field of view is approximately 3 by 2 mm. **F,** photomicrograph of wackestone containing ostracods and gastropods. Field of view is approximately 3 by 2 mm.

Depositional model

The Yeso depositional system is most analogous to the modern west coast of the Persian Gulf (Evans et al., 1969; Kendall and Skipworth, 1969; Schneider, 1975). The most landward lithofaces belt was composed of eolian sand (red siltstone–sandstone lithofacies). The predominance of climbing wind ripples suggests that the Yeso eolian sand lithofacies belt was similar to modern eolian sand sheets described by Fryberger et al. (1979). The paucity of large-scale crossbeds, indicative of dunes, many have been the result of low-velocity regional winds or slow sedimentation rates because of an inadequate supply of sand. Another possibility, which applies to the eolian sand sheet at Colorado National Monument (Fryberger et al., 1979), is that the eolian sand sheet in the southern Caballo Mountains was marginal to an eolian dune field that has yet to be recognized or that was removed by post-Yeso erosion. Locally within the eolian sand sheet were small playa lakes, which periodically precipitated halite (green sandstone lithofacies).

As the eolian sand sheet approached the shoreline, the sediment was increasingly affected by marginal-marine processes, including a greater degree of bioturbation and the formation of gypsum cements and halite cubes. The latter features probably resulted from capillary draw of hypersaline groundwater. Occasionally the eolian sand sheet may have been drowned, giving rise to intraformational folds attributable to water-escape mechanisms. This type of eolian sand is common in the red siltstone–dolomite and sandstone–limestone members.

Yeso tidal-flat sediment consisted of bioturbated and desiccated carbonate mud and peloids. Locally, peloids were transported by low-velocity currents, producing asymmetrical ripple cross-laminae. Algal (cyanobacteria) mats and mounds were an important component of the tidal flat and are responsible for cryptalgal laminae, LLH stromatolites, and fenestral fabric (Kendall and Skipworth, 1968; Shinn, 1968; Evans et al., 1969; Schneider, 1975). Because dolomite is restricted to the tidal-flat environment and is interbedded with gypsum and gypsiferous sandstone, dolomitization probably occurred in contact with hypersaline groundwater within a few thousand years or less after deposition, as it has along the coast of the Persian Gulf (Illing et al., 1965). In addition, some beds of white sandstone, particularly those displaying oscillation ripples, also may have been deposited on the tidal flat.

A variety of sediment was deposited in the subtidal belt of the Yeso depositional system. Closest to the shoreline was a lagoon, which was protected from the open ocean by oolite shoals. Abnormal salinity and/or poor circulation inhibited colonization by normal-marine fauna, resulting in deposition of carbonate mud with variable amounts of peloids, ostracods, foraminifera, and gastropods. A few scattered oolites floating in a micrite matrix also suggest that periodically they were washed into the lagoon from the oolite shoals by storms or strong tides. Occasionally the lagoon became hypersaline and precipitated gypsum, particularly during deposition of the red siltstone–dolomite member in the eastern part of the study area.

Seaward of the lagoon and oolite shoals, normal-marine conditions favored a highly diverse fauna. Especially diagnostic of this environment are filter feeders, such as brachiopods, stalked echinoderms, bryozoa, and corals (Fig. 4e). The presence of micrite matrix in these open-marine limestones, however, indicates an environment of low current energy, probably below normal wave base.

Depositional cycles

The Yeso Formation in the southern Caballo Mountains displays cyclic sedimentation on two scales. The larger scale cycle consists of a transgression followed by a regression. The transgression is recorded by the change from predominantly eolian deposits of the Meseta Blanca Member to mixed eolian–tidal flat–subtidal sediment of the red siltstone–dolomite member (Fig. 2). Transgression culminated with subtidal, open-marine sedimentation of the limestone member. A subsequent regression is indicated by a return to mixed eolian–tidal flat–subtidal sedimentation of the sandstone–limestone member (Fig. 2).

Superimposed on the large-scale cycle are smaller scale transgressive–regressive cycles that are 0.5 to 10 m thick. These cycles can be identified only in those members that consist of interbedded eolian, tidal-flat, and subtidal sediments, such as the red siltstone–dolomite and sandstone–limestone members. The most common cycles are simple alternations of lithofacies with sharp contacts, such as dolomite–limestone, dolomite–gypsum, and white sandstone–dolomite. Also common is the symmetrical cycle: red or white sandstone–dolomite–limestone–dolomite–red or white sandstone (Fig. 3).

There are several possibilities for the origin of depositional cycles in the Yeso Formation, including eustatic sea-level changes, changes in detrital sediment yield due to paleoclimatic fluctuations, interplay between the rate of basin subsidence and rate of carbonate production, and lateral shifting of complex lithofacies belts. These models are summarized by Langbein and Schumm (1958), Wilkinson (1982), James (1984) and Koerschner and Read (1989). It is beyond the scope of this study to distinguish the relative roles of these variables. In order to do this, it is necessary to correlate cycles throughout the basin, as well as between basins of different geographic areas. This study provides the first step in this process.

ACKNOWLEDGMENTS—This study was funded by a grant from the New Mexico Bureau of Mines and Mineral Resources. Travel expenses for Dr. Suguio were provided by the University of Sao Paulo and the Interamerican Development Bank. F. E. Kottlowski, M. Elrick, and R. E. Clemons read an earlier version of this paper and made helpful suggestions for its improvement.

References

Ahlbrandt, T. S., Andrews, S., and Gwynne, D. T., 1978, Bioturbation in eolian deposits: Journal of Sedimentary Petrology, v. 48, pp. 839–848.

Ball, M. M., 1967, Carbonate sand bodies of Florida and the Bahamas: Journal of Sedimentary Petrology, v. 37, pp. 556–591.

Bosellini, A., and Hardie, L. A., 1973, Depositional theme of a marginal marine evaporite: Sedimentology, v. 20, pp. 5–27.

Evans, G., Schmidt, V., Bush, P., and Nelson, H., 1969, Stratigraphy and geologic history of The Sabkha, Abu Dhabi, Persian Gulf: Sedimentology, v. 12, pp. 145–159.

Fryberger, S. G., and Schenk, C., 1981, Wind sedimentation tunnel experiments on the origins of aeolian strata: Sedimentology, v. 28, pp. 805–821.

Fryberger, S. G., Ahlbrandt, T. S., and Andrews, S., 1979, Origin, sedimentary features, and significance of low-angle eolian "sand sheet" deposits, Great Sand Dunes National Monument and vicinity, Colorado: Journal of Sedimentary Petrology, v. 49, pp. 733–746.

Harms, J. C., Southard, J. B., Spearing, D. R., and Walker, R. G., 1975, Depositional environments as interpreted from primary sedimentary structures and stratification sequences: Society of Economic Paleontologists and Mineralogists, Short Course no. 2, 161 pp.

Hunter, R. E., 1977, Basic types of stratification in small eolian dunes: Sedimentology, v. 24, pp. 361–387.

Illing, R. V., Wells, A. J., and Taylor, J. C. M., 1965, Penecontemporary dolomite in the Persian Gulf: Society of Economic Paleontologists and Mineralogists, Special Publication 13, pp. 89–111.

James, N. P., 1984, Shallowing-upward sequences in carbonates: Geoscience Canada, Reprint Series 1, 2nd edition, pp. 213–228.

Kelley, V. C., and Silver, C., 1952, Geology of the Caballo Mountains: University of New Mexico, Publications in Geology no. 4, 286 pp.

Kendall, A. C., 1984, Evaporites; *in* Walker, R. G. (ed.), Facies models: Geoscience Canada, Reprint Series 1, 2nd edition, pp. 259–296.

Kendall, G. St. C., and Skipworth, Sir P. A. d'E., 1968, Recent algal mats of a Persian Gulf lagoon: Journal of Sedimentary Petrology, v. 38, pp. 1040–1058.

Kendall, G. St. C., and Skipworth, Sir P. A. d'E., 1969, Holocene shallow-water carbonate and evaporite sediments of Khor al Basam, Abu Dhabi, southwest Persian Gulf: American Association of Petroleum Geologists, Bulletin, v. 53, pp. 841–869.

Koerschner, W. F., III, and Read, J. F., 1989, Field and modelling studies of Cambrian carbonate cycles, Virginia Appalachians: Journal of Sedimentary Petrology, v. 59, pp. 654–687.

Kottlowski, F. E., 1963, Paleozoic and Mesozoic strata of southwestern and south-central New Mexico: New Mexico Bureau of Mines and Mineral Resources, Bulletin 79, 100 pp.

(Continued on p. 59)

rocks of the Sandia Mountains, New Mexico: Geological Society of America, Bulletin, v. 90, Part I, p. 138–140, Part II, p. 349–380.
Laughlin, A. W., and Eddy, A. C., 1977, Petrography and geochemistry of Precambrian core samples from GT–2 and EE–1: Los Alamos Scientific Laboratory, Rept. LA–6930–MS, 50 pp.
Laughlin, A. W., Eddy, A. C., Laney, R., and Aldrich, M. J., Jr., 1983, Geology of the Fenton Hill, New Mexico, hot dry rock site: Journal of Volcanology and Geothermal Research, v. 15, pp. 21–41.
Majumdar, A., 1985, Geochronology, geochemistry, and petrology of the Precambrian Sandia granite, Albuquerque, New Mexico: Unpublished Ph.D. dissertation, Louisiana State Univ., 212 pp.
Steiger, R. H., and Wasserburg, G. J., 1969, Comparative U–Th–Pb systematics in 2.7 × 10^9 yr plutons of different geologic histories: Geochimica et Cosmochimica Acta, v. 33, pp. 1213–1232.
Taggert, J. E., and Brookins, D. G., 1975, Rb–Sr whole rock age determinations for Sandia granite and Cibola gneiss, New Mexico: Isochron/West, no. 12, pp. 5–8.
Tilton, G. R., Wetherill, G. W., and Davis, G. L., 1962, Mineral ages from the Wichita and Arbuckle Mountains, Oklahoma and the St. Francis Mountains, Missouri: Journal of Geophysical Research, v. 65, pp. 4011–4020.
Tilton, G. R., and Grunenfelder, M. H., 1968, Sphene: uranium–lead ages: Science, v. 159, pp. 1458–1461.
Woodward, L. A., and Callender, J. F., 1977, Tectonic framework of the San Juan Basin: New Mexico Geological Society, Guidebook to 28th Field Conference, pp. 209–212.
Zartman, R. E., 1979, Uranium, thorium, and lead concentrations and lead isotopic composition of biotite granodiorite (sample 9527–2b) from LASL drill hole GT–2: Los Alamos Scientific Laboratory, Rept. LA–7923–MS, 18 pp.

Yeso Formation

(*Continued from p. 49*)

Kottlowski, F. E., 1965, Sedimentary basins of south-central and southwestern New Mexico: American Association of Petroleum Geologists, Bulletin, v. 49, pp. 2120–2139.
Kottlowski, F. E., Flower, R. H., Thompson, M. L., and Foster, R. W., 1956, Stratigraphic studies of the San Andres Mountains, New Mexico: New Mexico Bureau of Mines and Mineral Resources, Memoir 1, 132 pp.
Langbein, W. B., and Schumm, S. A., 1958, Yield of sediment in relation to mean annual precipitation: American Geophysical Union, Transactions, v. 39, pp. 1076–1084.
Nelson, E. P., 1986, Geology of the Fra Cristobal Range, south-central New Mexico: New Mexico Geological Society, Guidebook to 37th Field Conference, pp. 83–91.
Sarg, J. F., 1981, Petrology of the carbonate–evaporite facies transition of the Seven Rivers Formation (Guadalupian, Permian), southeast New Mexico: Journal of Sedimentary Petrology, v. 51, pp. 73–96.
Schneider, J. F., 1975, Recent tidal deposits, Abu Dhabi, UAE, Arabian Gulf; *in* Ginsburg, R. N. (ed.), Tidal deposits: New York, Springer–Verlag, pp. 209–214.
Seager, W. R., and Mack, G. H., in press, Geology of McLeod Tank quadrangle, Sierra County, New Mexico: New Mexico Bureau of Mines and Mineral Resources, Geologic Map.
Shinn, E. A., 1968, Practical significance of birdseye structures in carbonate rocks: Journal of Sedimentary Petrology, v. 38, pp. 215–223.
Shinn, E. A., 1983, Tidal flat environment; *in* Scholle, P. A., Bebout, D. G., and Moore, C. H. (eds.), Carbonate depositional environments: American Association of Petroleum Geologists, Memoir 33, pp. 172–210.
Thode, H. G., Monster, J., and Dunford, H. B., 1961, Sulfur isotope geochemistry: Geochimica et Cosmochimica Acta, v. 25, pp. 159–174.
Wilkinson, B. R., 1982, Cyclic cratonic carbonates and Phanerozoic calcite seas: Journal of Geological Education, v. 30, pp. 189–203.
Wilpolt, R. H., and Wanek, A. A., 1951, Geology of the region from Socorro and San Antonio east to Chupadera Mesa, Socorro County, New Mexico: U.S. Geological Survey, Oil and Gas Investigations, Preliminary Map OM 121.

Grassy Lookout quadrangle

(*Continued from p. 54*)

References

Aldrich, M. J., Jr., Chapin, C. E., and Laughlin, A. W., 1986, Stress history and tectonic development of the Rio Grande rift, New Mexico: Journal of Geophysical Research, v. 91, pp. 6199–6211.
Chamberlin, R. M., 1983, Cenozoic domino-style crustal extension in the Lemitar Mountains, New Mexico—a summary: New Mexico Geological Society, Guidebook to 34th Field Conference, pp. 111–118.
Chapin, C. E., 1979, Evolution of the Rio Grande rift—a summary; *in* Riecker, R. E. (ed.), Rio Grande rift: tectonics and magmatism: American Geophysical Union, pp. 1–5.
Chapin, C. E., 1989, Volcanism along the Socorro accommodation zone, Rio Grande rift, New Mexico; *in* Field excursions to volcanic terranes in the western United States, Volume I: Southern Rocky Mountain region: New Mexico Bureau of Mines and Mineral Resources, Memoir 46, pp. 46–57.
Chapin, C. E., Chamberlin, R. M., Osburn, G. R., Sanford, A. R., and White, D. L., 1978, Exploration framework of the Socorro geothermal area, New Mexico; *in* Chapin, C. E., and Elston, W. E. (eds.), Field guide to selected cauldrons and mining districts of the Datil–Mogollon volcanic field, New Mexico: New Mexico Geological Society, Special Publication 7, pp. 115–129.
Deal, E. G., 1973, Geology of the northern part of the San Mateo Mountains, Socorro County, New Mexico—a study of a rhyolite ash-flow tuff cauldron and the role of laminar flow in ash-flow tuffs: Unpublished PhD dissertation, University of New Mexico, 136 pp.
Deal, E. G., and Rhodes, R. C., 1976, Volcano-tectonic structures in the San Mateo Mountains, Socorro County, New Mexico; *in* Elston, W. E., and Northrop, S. A. (eds.), Cenozoic volcanism in southwestern New Mexico: New Mexico Geological Society, Special Publication 5, pp. 51–56.
Donze, M. A., 1980, Geology of the Squaw Peak area, Magdalena Mountains, Socorro County, New Mexico: New Mexico Bureau of Mines and Mineral Resources, Open-file Report 123, 131 pp.
Eggleston, T. L., 1982, Geology of the central Chupadera Mountains, Socorro County, New Mexico: New Mexico Bureau of Mines and Mineral Resources, Open-file Rept. 141, 162 pp.
Elston, W. E., 1989, Overview of the Mogollon–Datil volcanic field; *in* Chapin, C. E., and Zidek, J. (eds.), field excursions to volcanic terranes in the western United States, Volume I: Southern Rocky Mountain region: New Mexico Bureau of Mines and Mineral Resources, Memoir 46, pp. 43–46.
Elston, W. E., Damon, P. E., Coney, P. J., Rhodes, R. C., Smith, E. I., and Bikerman, Michael, 1973, Tertiary volcanic rocks, Mogollon–Datil province, New Mexico, and surrounding region: K-Ar dates, patterns of eruption, and periods of mineralization: Geological Society of America, Bulletin, v. 84, pp. 2259–2274.
Ferguson, C. A., 1986, Geology of the east-central San Mateo Mountains, Socorro County, New Mexico: New Mexico Bureau of Mines and Mineral Resources, Open-file Report 252, 134 pp., 4 plates.
Ferguson, C. A., 1988, Geology of the Tenmile Hill 7½-min quadrangle, Socorro County, New Mexico: New Mexico Bureau of Mines and Mineral Resources, Open-file Report 283, 21 pp., 2 plates.
Ferguson, C. A., 1990, Geology of the Grassy Lookout 7½-min quadrangle, Socorro County, New Mexico: New Mexico Bureau of Mines and Mineral Resources, Open-file Report 366, 41 pp., 3 plates.
Gile, L. H., Hawley, J. W., and Grossman, R. B., 1981, Soils and geomorphology in the Basin and Range area of southern New Mexico—guidebook to the Desert Project: New Mexico Bureau of Mines and Mineral Resources, Memoir 39, 222 pp.
Lipman, P. W., 1976, Caldera-collapse breccias in the western San Juan Mountains, Colorado: Geological Society of America, Bulletin, v. 87, pp. 1397–1410.
Machette, M. N., 1987, Preliminary assessment of Quaternary faulting near Truth or Consequences, New Mexico: U.S. Geological Survey, Open-file Report 87–652, 40 pp.
McIntosh, W. C., 1989a, Timing and distribution of ignimbrite volcanism in the Eocene–Miocene Mogollon–Datil volcanic field, *in* Chapin, C. E., and Zidek, J. (eds.), Field excursions to volcanic terranes in the western United States, Volume I: Southern Rocky Mountain region: New Mexico Bureau of Mines and Mineral Resources Memoir 46, pp. 58–59.
McIntosh, W. C., 1989b, Ages and distribution of ignimbrites in the Mogollon–Datil volcanic field, southwestern New Mexico—a stratigraphic framework: Unpublished PhD dissertation, New Mexico Institute of Mining and Technology.
McIntosh, W. C., Sutter, J. F., Chapin, C. E., Osburn, G. R., and Ratté, J. C., 1986, A stratigraphic framework for the eastern Mogollon–Datil volcanic field based on paleomagnetism and high-precision $^{40}Ar/^{39}Ar$ dating of ignimbrites—a progress report: New Mexico Geological Society, Guidebook to 37th Field Conference, pp. 183–195.
Morgan, P., Seager, W. R., and Golombek, M. P., 1986, Cenozoic thermal, mechanical, and tectonic evolution of the Rio Grande rift: Journal of Geophysical Research, v. 91., pp. 6263–6276.
Osburn, G. R., and Chapin, C. E., 1983, Nomenclature for Cenozoic rocks of northeast Mogollon–Datil volcanic field, New Mexico: New Mexico Bureau of Mines and Mineral Resources, Stratigraphic Chart 1, 7 pp., 1 sheet.
Osburn, G. R., and Ferguson, C. A., 1986, Redefinition of the Mt. Withington cauldron (abs.): New Mexico Geology, v. 8, p. 98.
Smith, R. L., and Bailey, R. A., 1968, Resurgent cauldrons; *in* Studies in volcanology—a memoir in honor of Howell Williams: Geological Society of America, Memoir 116, pp. 613–662.
Stewart, J. H., 1980, Regional tilt patterns of late Cenozoic basin-range fault blocks, western United States: Geological Society of America, Bulletin, v. 91, pp. 460–464.
Wright, J. V., and Walker, G. P., 1977, The ignimbrite source problem: significance of a co-ignimbrite lag-fall deposit: Geology, v. 5, pp. 729–732.
Zoback, M. L., Anderson, R. E., and Thompson, G. A., 1981, Cainozoic evolution of the state of stress and the style of tectonism of the Basin and Range province of the western United States: Philosophical Transactions of the Royal Society of London, v. 300, ser. A, pp. 407–434.